

## ELECTRONIC SUPPLEMENTARY INFORMATION

### Grafting density and thickness of polythiophene-based brushes determine orientation, conjugation length and stability of the grafted chains

K. Wolski,<sup>a</sup> A. Gruskiewicz,<sup>a</sup> M. Wytrwał-Sarna,<sup>b</sup> A. Bernasik,<sup>b,c</sup> and S. Zapotoczny<sup>a†</sup>

<sup>a</sup>Jagiellonian University, Faculty of Chemistry, Gronostajowa 2, 30-387 Krakow, Poland

<sup>b</sup>AGH University of Science and Technology, Academic Centre for Materials and Nanotechnology, al. A. Mickiewicza 30, 30-059, Krakow, Poland

<sup>c</sup>AGH University of Science and Technology, Faculty of Physics and Applied Computer Science, al. A. Mickiewicza 30, 30-059 Krakow, Poland

†Corresponding author. E-mail: [zapotocz@chemia.uj.edu.pl](mailto:zapotocz@chemia.uj.edu.pl)

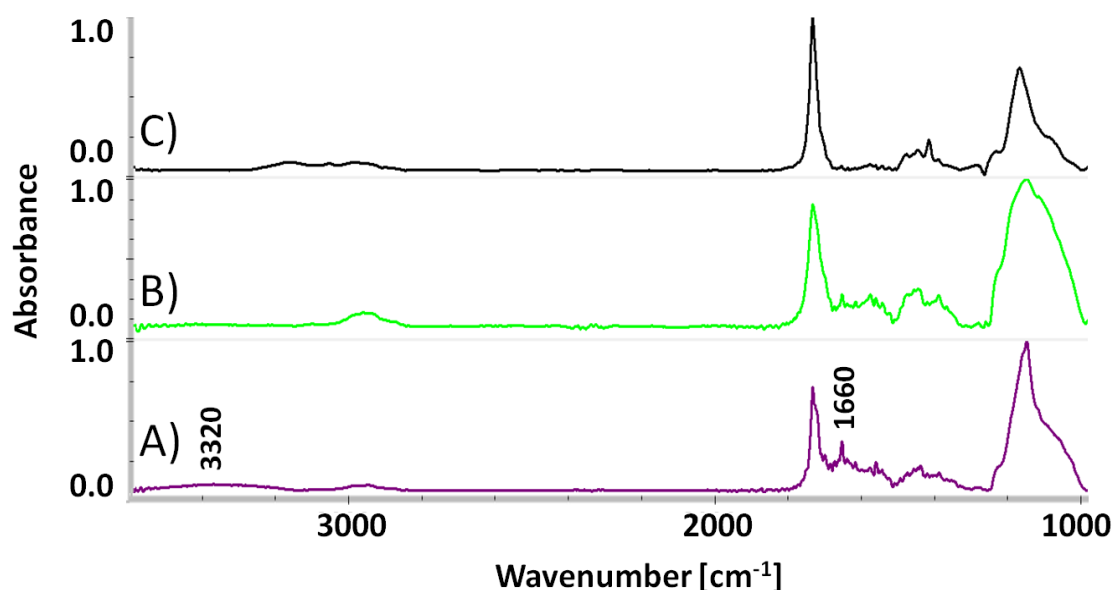


**Figure S1.** FTIR p-polarized spectra of conjugated PMTM brushes after template polymerization: A) kept for one hour in the doped state under ambient conditions before dedoping process, B) immediately dedoped under ambient conditions, C) immediately dedoped under red light.

**Table S1.** Atomic concentration determined by XPS for conjugated PMTM brushes that were differently purified after oxidative polymerization with  $\text{FeCl}_3$  either under laboratory white light (l.l.) or red light (r.l.).

Sample	C1s			C1s total	O1s			O1s total	S2p
	C-C,H,S	C-O	O-C=O		C-O	C=O	Oxide		
PMTM_100l.l.	55.5	13.2	6.7	75.4	11.3	7.7	1.4	20.4	4.3
PMTM_100r.l.	59.7	8.3	7.3	75.3	10.3	8.5	0.0	18.8	6.0
PMTM_80r.l.	58.8	9.0	8.1	75.8	10.7	7.7	0.0	18.4	5.8
PMTM_60r.l.	57.1	11.5	6.4	75.0	11.1	8.0	0.0	19.1	5.9
Measurements done after 1 week storage under ambient conditions									
PMTM_100r.l.	55.7	11.3	7.4	74.4	12.4	7.8	0.0	20.2	5.4
PMTM_80r.l.	55.0	12.3	7.6	74.9	11.8	7.9	0.0	19.7	5.4
PMTM_60r.l.	54.0	11.9	8.5	74.1	13.2	7.9	0.0	21.1	4.8

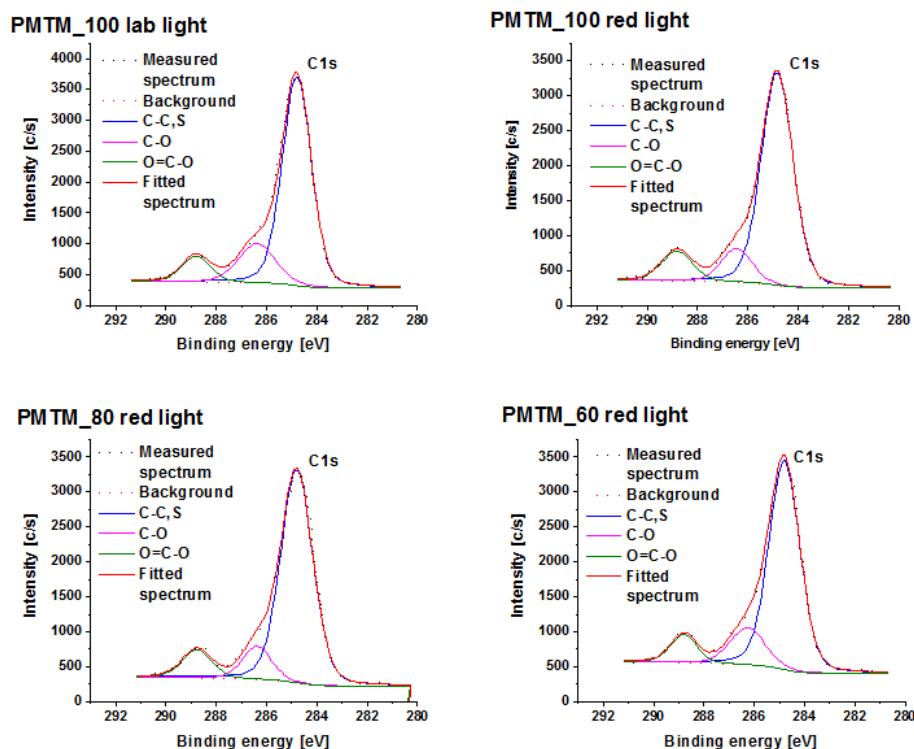


**Figure S2.** C1s XPS spectra (together with respective fitted bands) of freshly prepared PMTM brushes with different grafting densities (purified under ambient and red light).

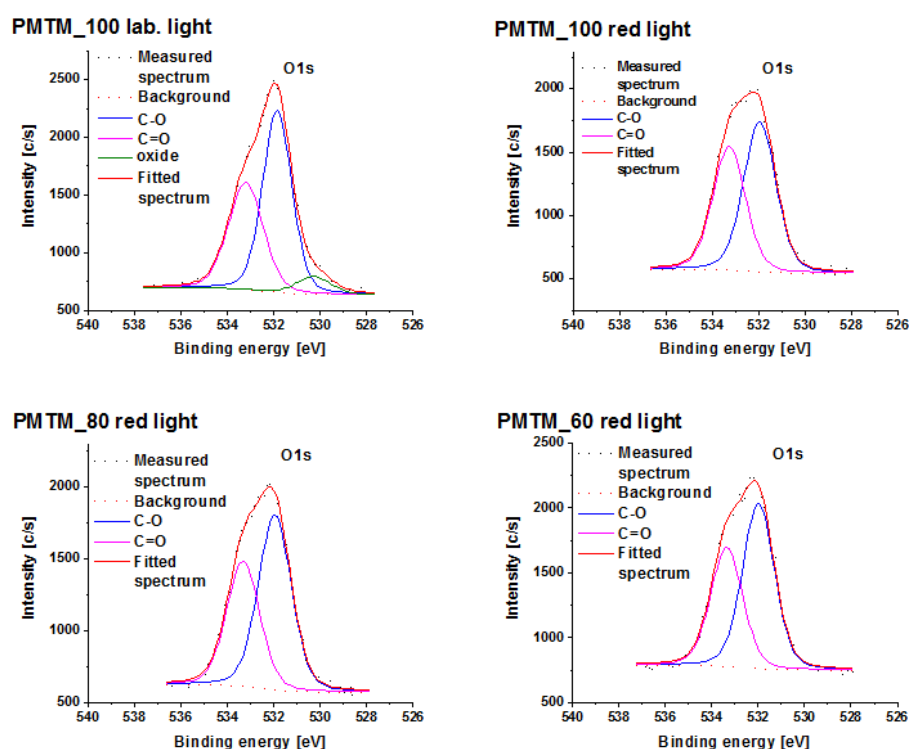


**Figure S3.** O1s XPS spectra (together with respective fitted bands) of freshly prepared PMTM brushes with different grafting densities (purified under ambient and red light).

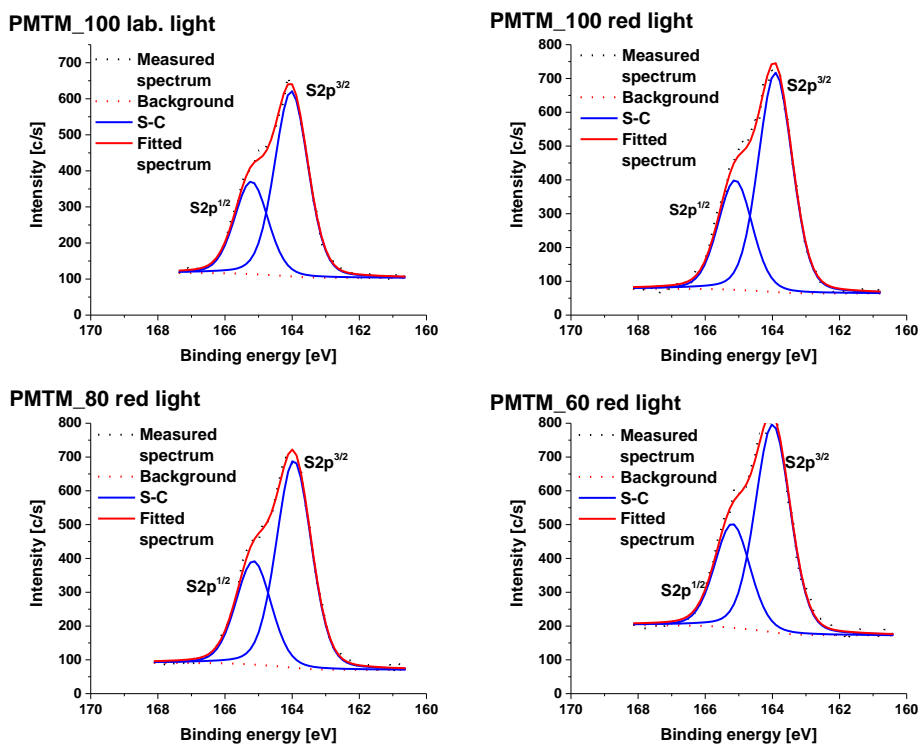


**Figure S4.** S2p XPS spectra (together with respective fitted bands) of freshly prepared PMTM brushes with various grafting densities (purified under ambient and red light).

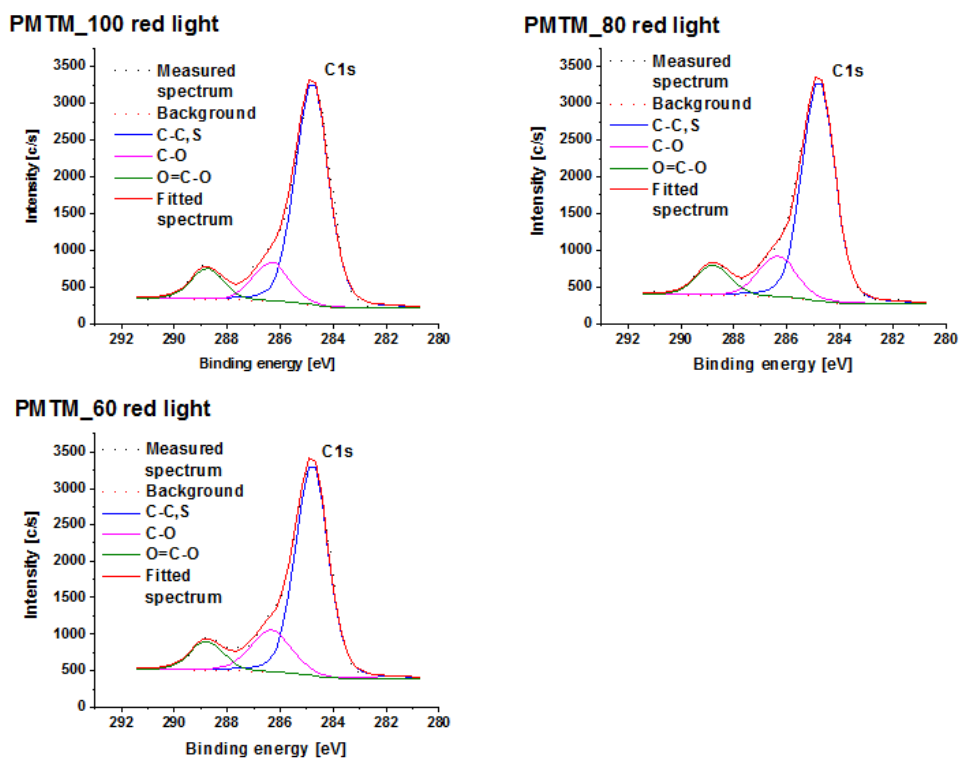


**Figure S5.** C1s XPS spectra (together with respective fitted bands) of PMTM brushes with various grafting densities captured after 1 week storage of the samples under ambient light.

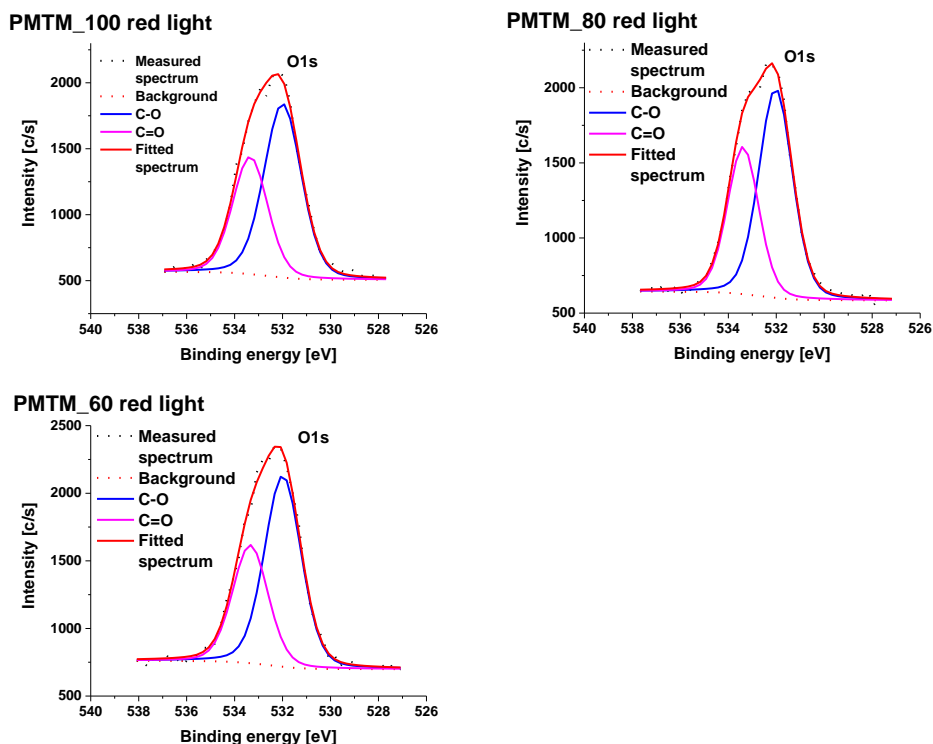


**Figure S6.** O1s XPS spectra (together with respective fitted bands) of PMTM brushes with various grafting densities captured after 1 week storage of the samples under ambient light.

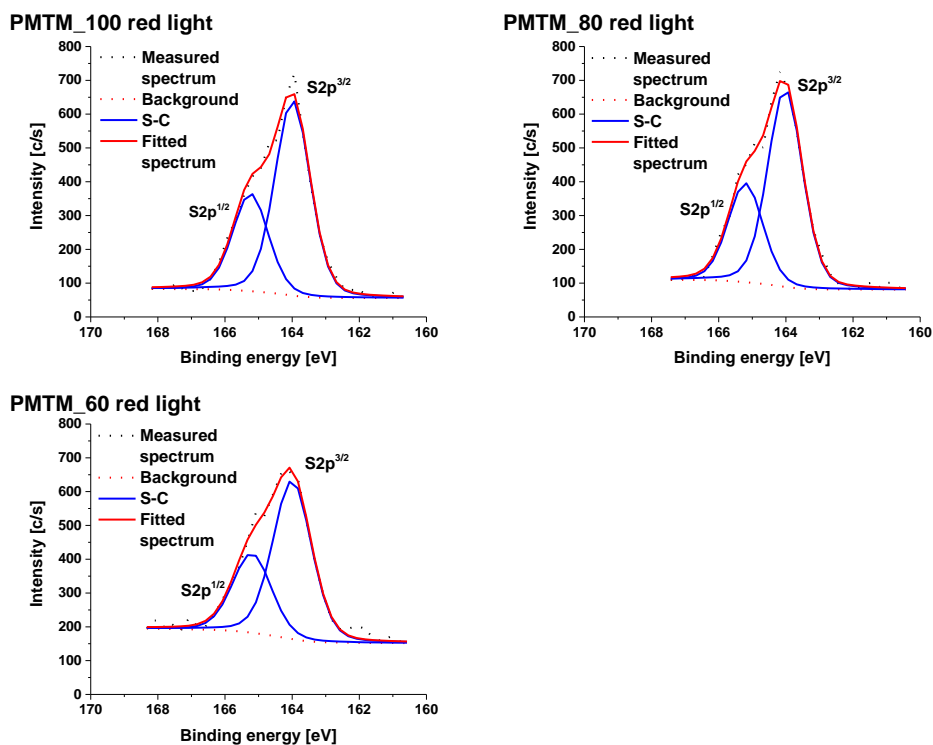


**Figure S7.** S2p XPS spectra (together with respective fitted bands) of PMTM brushes with various grafting densities captured after 1 week storage of the samples under ambient light.

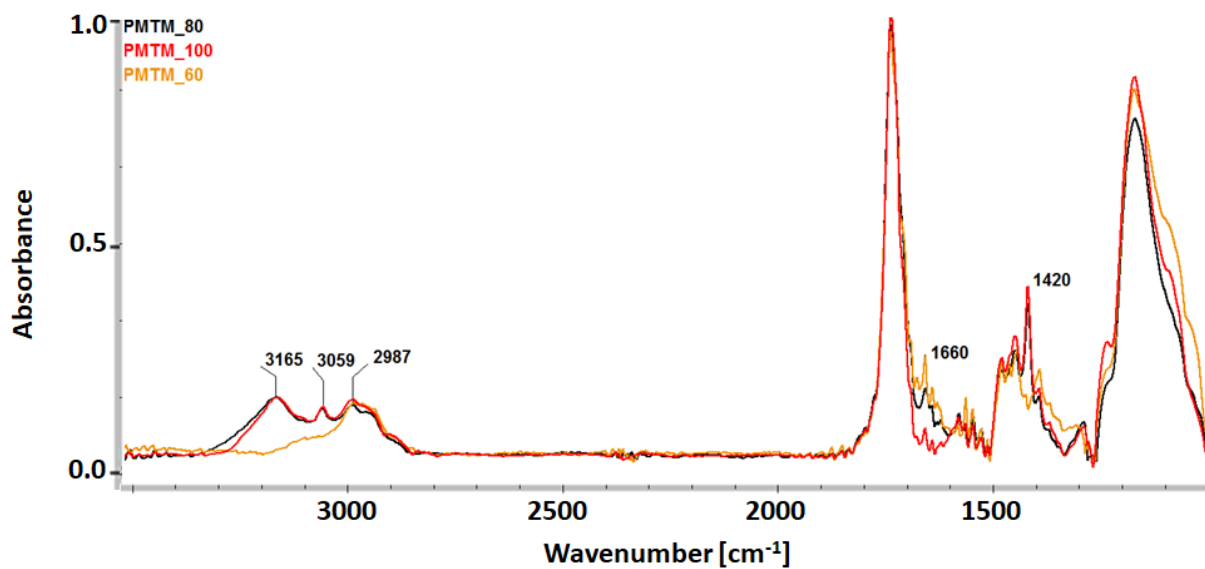


**Figure S8.** Normalized FTIR spectra captured immediately after oxidative template polymerization of PMTM brushes with various grafting densities (purification performed under red light).

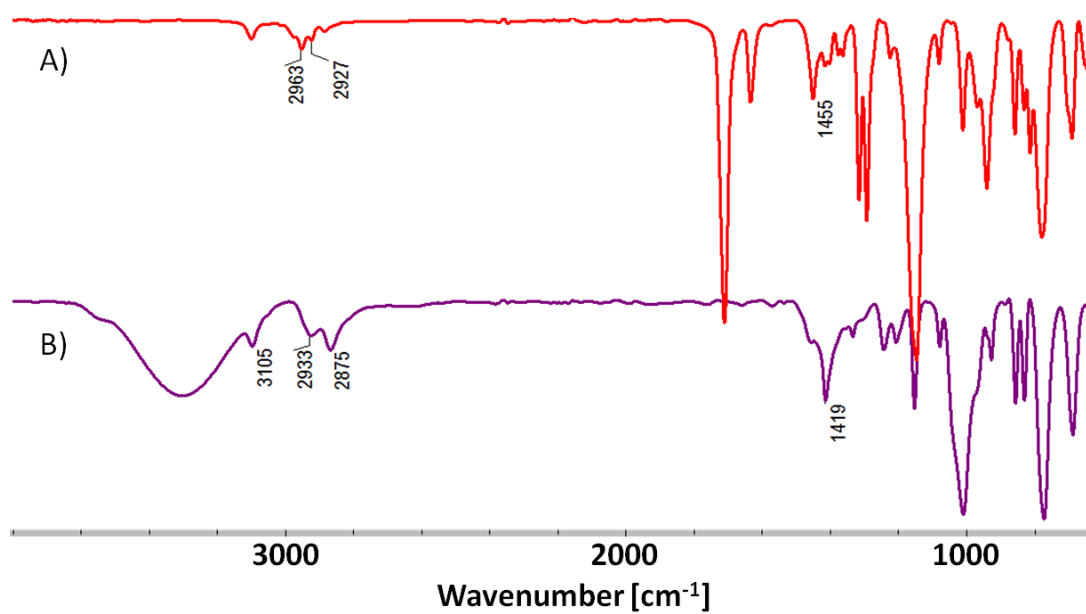


**Figure S9.** FTIR transmittance spectra of: A) MTM monomer and B) 3-thiophenemethanol.

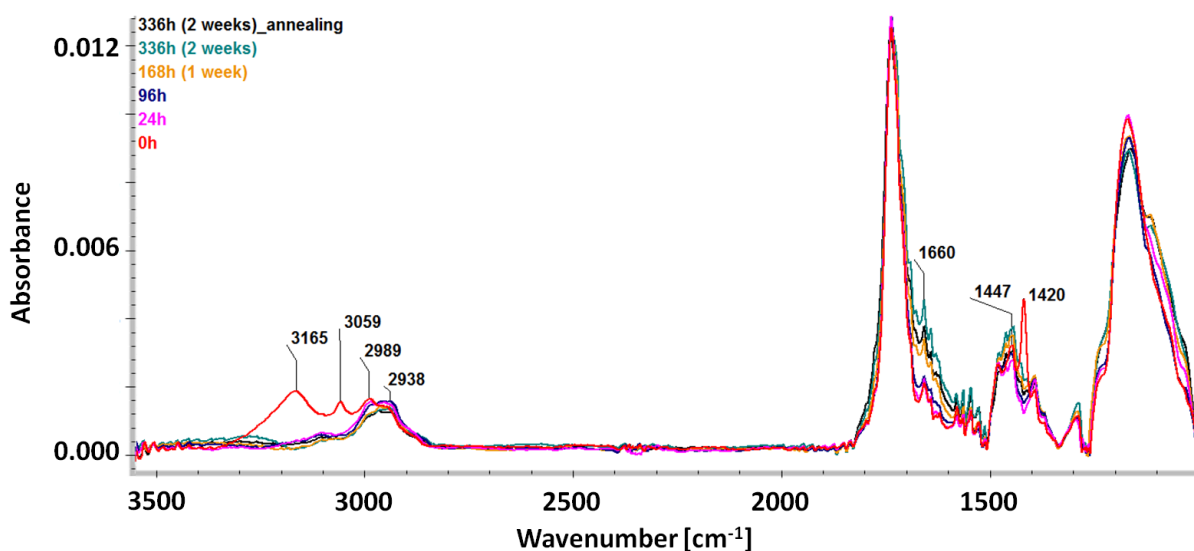


**Figure S10.** Normalized FTIR spectra of conjugated PMTM<sub>80</sub> brush captured after storage at given times under ambient conditions (purification performed under red light).

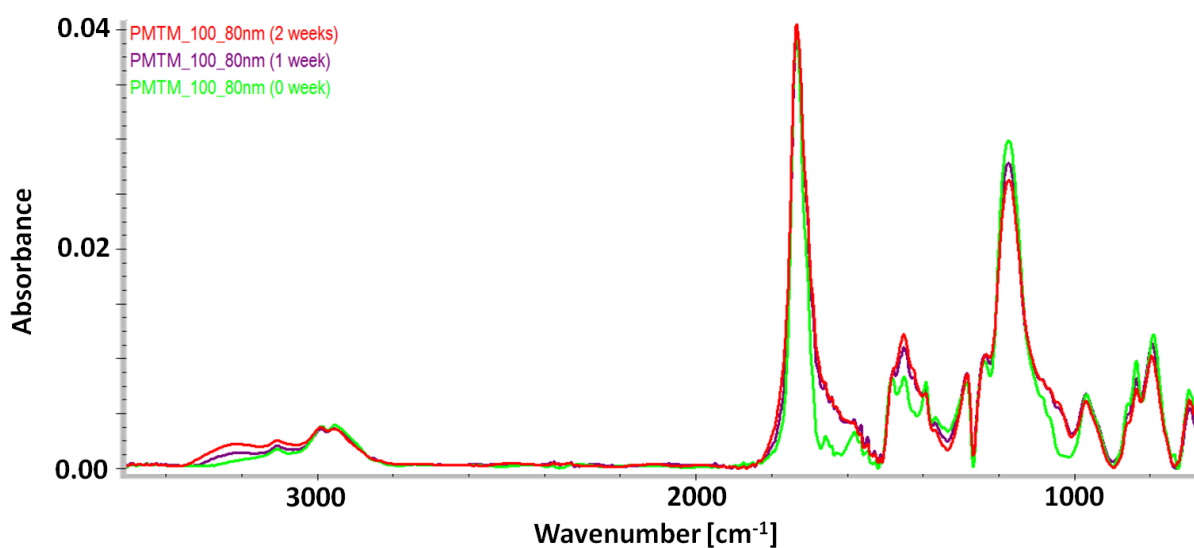


**Figure S11.** Normalized FTIR spectra of conjugated PMTM<sub>100\_80nm</sub> brush captured after storage at given times under ambient conditions (purification performed under red light).

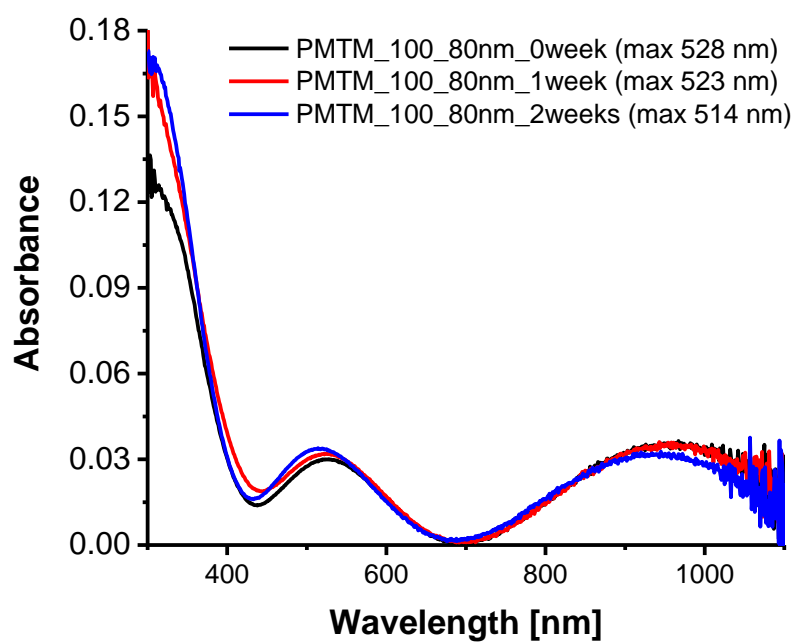


**Figure S12.** UV-VIS-NIR spectra of conjugated PMTM\_100\_80nm brush captured after storage at given times under ambient conditions (purification performed under red light).

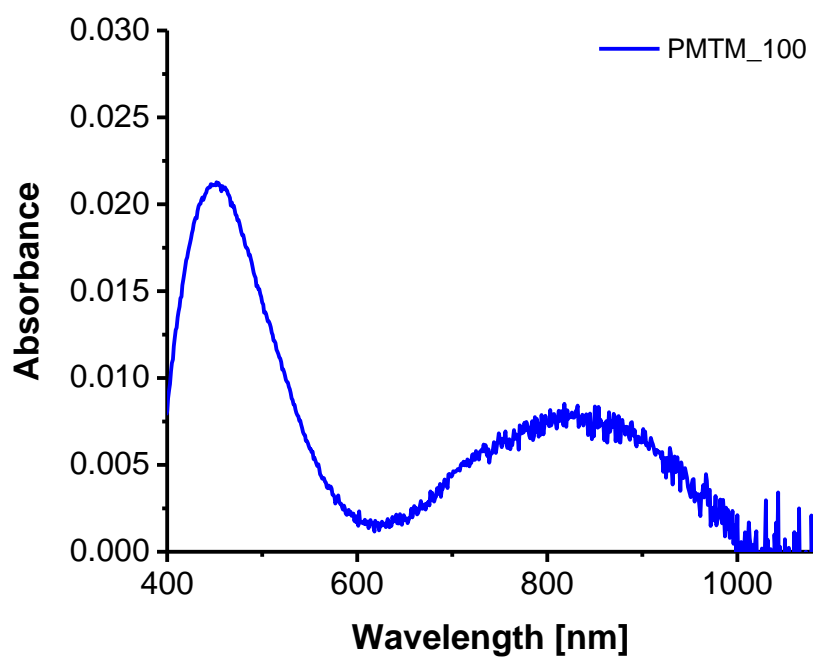


**Figure S13.** UV-VIS-NIR spectrum of conjugated PMTM\_100 brush (purification under red light).

### Copper(I) complexes with MTM monomer and different ligands

In order to test whether MTM monomer can form complex with copper(I), the solution of 0.125 ml MTM in 0.5 ml DMF (concentration 1.3 M) was transferred under argon to the vessel with 1.25 mg CuBr. The blank test with clean DMF (0.5 ml) transferred to the CuBr (1.25 mg) under the same conditions was also conducted. CuBr was completely dissolved in MTM solution after only a few minutes creating transparent pale green solution (fig. S14 B) while yellow CuBr/DMF mixture was turbid with undissolved CuBr (fig. S14 A). After oxidation of the mixture with one droplet of perhydrol the differences were even more pronounced (fig S14 C and D). Similar changes were noticed after exposure of the mixtures to air that leads to oxidation of Cu(I) to Cu(II). Much better solubility of CuBr in DMF containing MTM and the reported variations of colours clearly indicate that MTM monomer is able to complex copper ions.

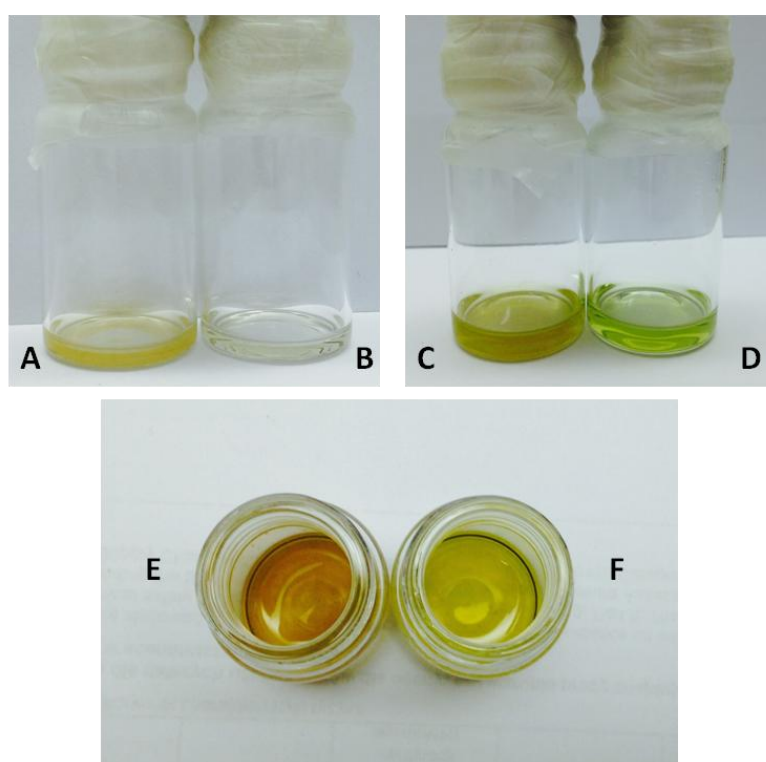


**Figure S14.** Pictures of: A) CuBr/DMF solution in argon atmosphere, B) CuBr/MTM/DMF solution in argon atmosphere, C) CuBr/DMF solution in argon atmosphere after oxidation, D) CuBr/MTM/DMF solution in argon atmosphere after oxidation, E) CuBr/DMF solution exposed to air , F) CuBr/MTM/DMF solution exposed to air.

In order to show competitive complexation between different ligands and MTM monomer, the solution of MTM (0.27 mmol)/ ligand (0.031 mmol)/ DMF (0.27 ml) was transferred under argon to the vessel containing 0.4 mg of CuBr. We noticed that the colors of the obtained mixture significantly differed for the used ligands. Transparent and dark green solution was observed for PMDETA (fig. S15 A), yellow-brown mixture for Me<sub>6</sub>TREN (fig. S15 B), and green solution for HMTETA (fig. S15 C). After oxidation in air different tints of green were observed in all the vials (fig. S15 D).

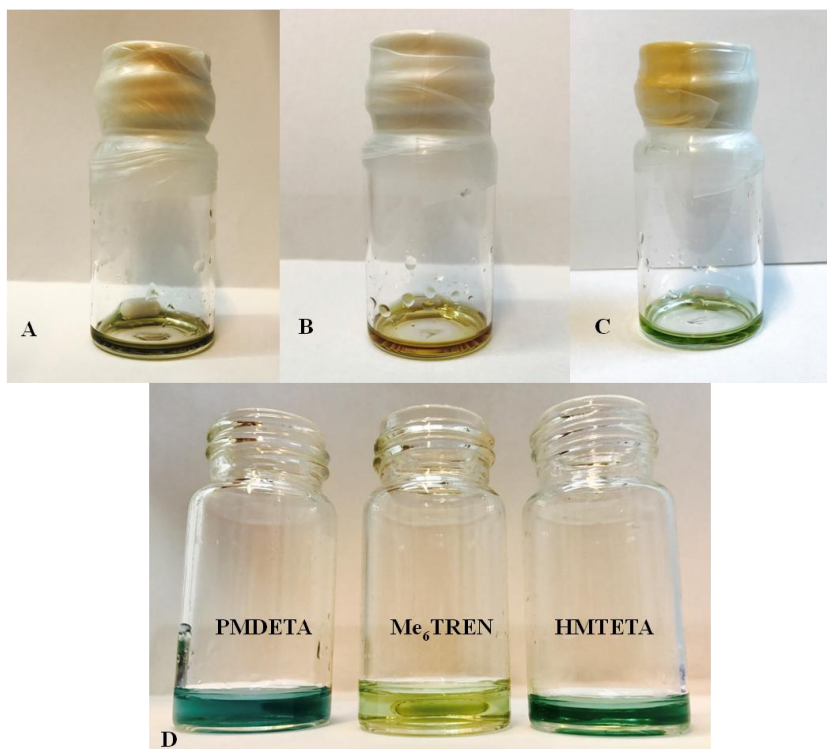


**Figure S15.** Pictures of: A) CuBr/MTM/PMDETA/DMF solution in argon atmosphere, B) CuBr/MTM/Me<sub>6</sub>TREN/DMF solution in argon atmosphere, C) CuBr/MTM/HMTETA/DMF solution in argon atmosphere, D) CuBr/MTM/ligand/DMF solutions after oxidation.

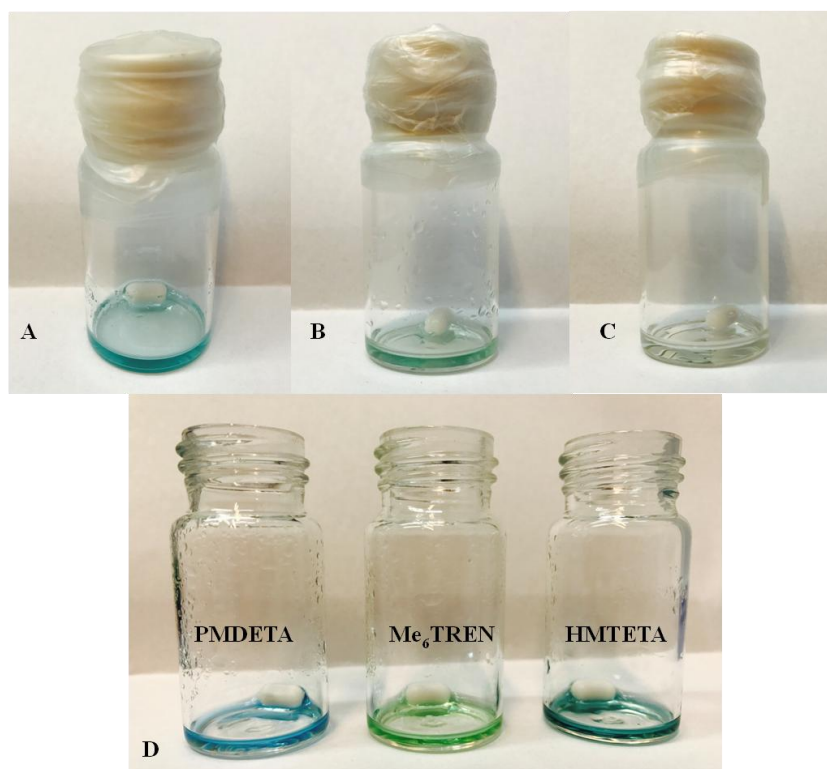


**Figure S16.** Pictures of: A) CuBr/PMDETA/DMF solution in argon atmosphere, B) CuBr/ Me<sub>6</sub>TREN/DMF solution in argon atmosphere, C) CuBr/HMTETA/DMF solution in argon atmosphere, D) CuBr/ligand/DMF solution after oxidation.

The respective solutions without the MTM monomer and the same concentrations of the ligands ( $c=0.1$  M) were also prepared (0.062 mmol ligand in 0.6 ml DMF was transferred under argon to the vessel with 1.25 mg CuBr). The solutions without MTM exhibited very much different colors than the solutions with MTM indicating some competing complexations of Cu(I) with MTM for all three studied ligands (fig. S16 A-C). Interestingly, after oxidation, the colors of created complexes with Cu(II) were similar to those one in the presence of MTM monomer (fig. S16 D).

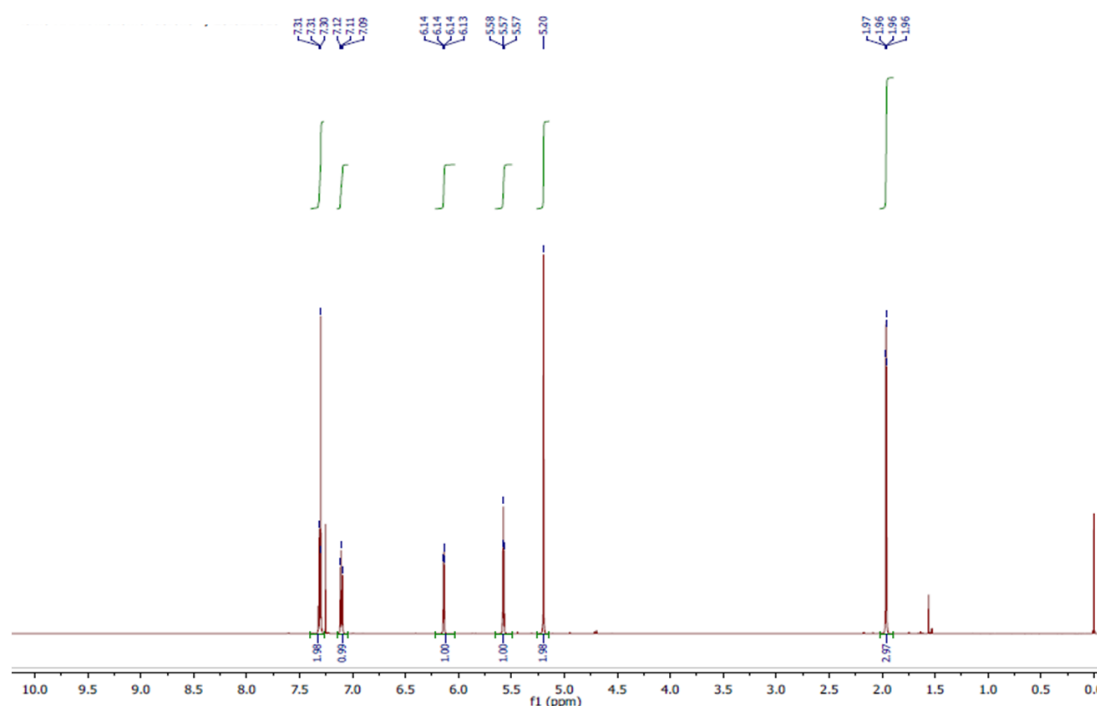


**Figure S17.**  $^1\text{H}$  NMR spectrum of MTM monomer (300 MHz,  $\text{CDCl}_3$ ):  $\delta$  7.31 (m, 2H), 7.11 (m, 1H), 6.14 (m, 1H), 5.58 (q,  $J = 1.6$ , 1H), 5.20 (s, 2H), 1.96 (dd,  $J = 1.6, 1.0$ , 3H).

### Estimation of PMTM brush grafting density

In order to estimate PMTM brush grafting density SI-ATRP was conducted in the presence of sacrificial initiator (ethyl 2-bromoisobutyrate, EtBIB). The molar ratios of reagents were as follows: EtBIB (0.6):  $\text{CuBr}_2$  (1): CuBr (10): HMTETA (37.5): MTM (1000). Molecular weight distribution of the PMTM formed in the solution above the formed brushes was determined using gel permeation chromatography (GPC). Under the applied SI-ATRP conditions, PMTM brushes with the dry thickness of  $9.9 \pm 0.8$  nm were obtained on ITO surface. GPC analysis of the PMTM obtained in the solution revealed:  $M_n = 14\,500$  g/mol,  $M_w = 22\,000$  g/mol, and dispersity,  $D = 1.52$  as determined using poly(methyl methacrylate) standards (see fig. S18). Grafting density ( $\sigma$ ) of PMTM brushes was calculated using simple formula (eq. 1):

$$\sigma = \frac{h \cdot d \cdot N_A}{M_n} \quad (1)$$

where:

h - dry brush thickness;  
d - polymer density;  
 $N_A$  - Avogadro constant;  
 $M_n$  - number average molecular weight.

PMTM density ( $1.3 \text{ g/cm}^3$ ) was assumed to be slightly higher than the monomer density ( $1.2 \text{ g/cm}^3$ ) as such trend is observed in many polymeric systems. The grafting density was found to be on the level of  $0.53 \text{ chain/nm}^2$ .

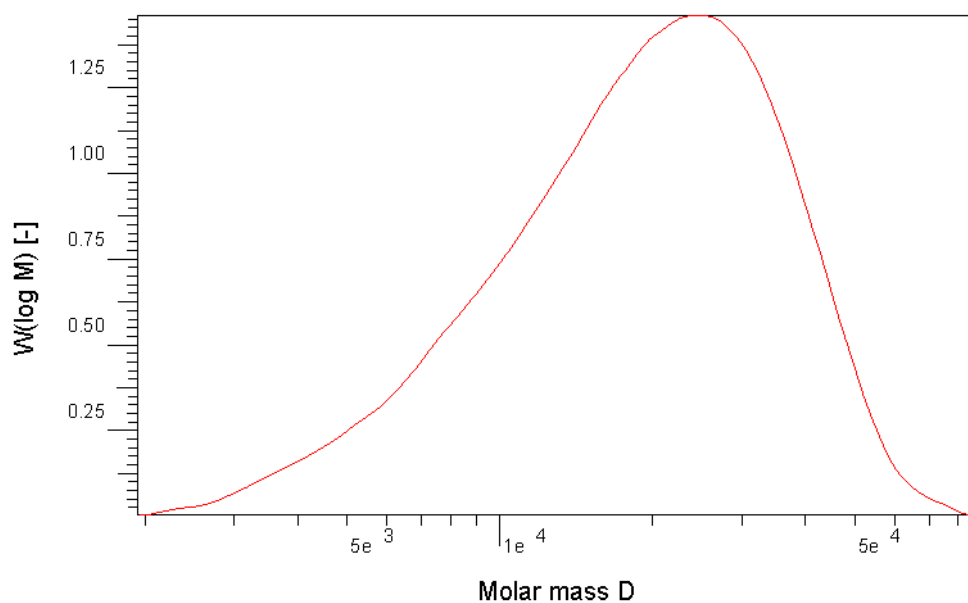


**Figure S18.** Molecular weight distribution of PMTM obtained in the solution during SI-ATRP with the sacrificial initiator.

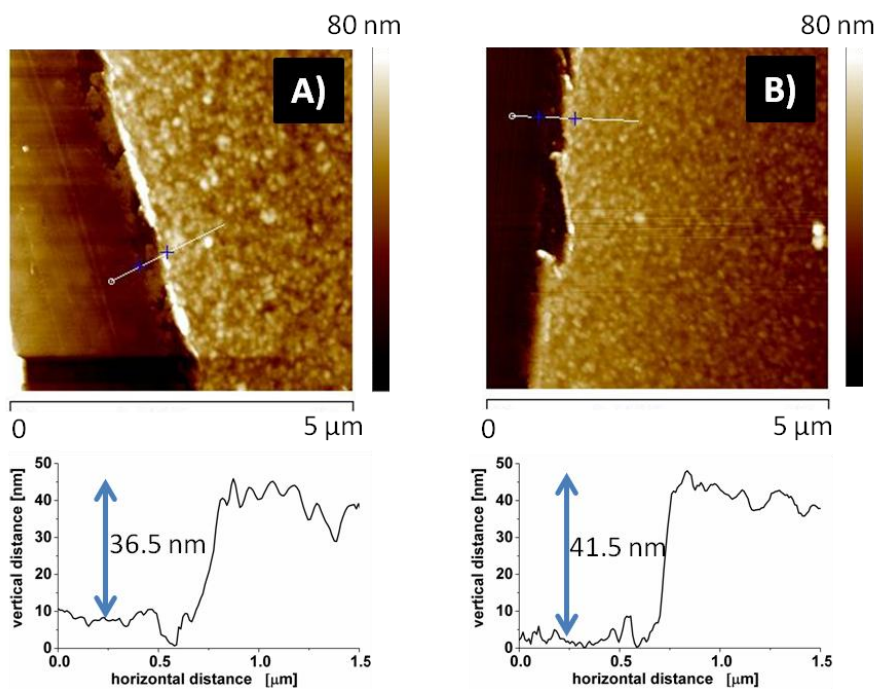


**Figure S19.** SI-ATRP of MTM monomer (reaction time 60 min) from specially designed ITO chip with ITO electrodes separated by glass surface. PMTM brushes formed on A) ITO electrode and B) neighboring glass surface.

#### FTIR characterization of ITO surface modified with ATRP initiator

In order to confirm attachment of ATRP initiator to ITO surface grazing-angle FTIR spectra were collected after each synthetic step (see fig. S20). FTIR spectrum captured for ITO decorated with APTES revealed the appearance of characteristic bands for amine groups at  $3274\text{ cm}^{-1}$  (N-H stretching vibrations in primary amines) and  $1582\text{ cm}^{-1}$  (scissor vibration of the  $\text{NH}_2$  terminal group). After reaction with BIB the previously observed bands disappeared while the bands at  $3329\text{ cm}^{-1}$  (N-H stretching in amide group),  $1657\text{ cm}^{-1}$  (C=O stretching (amide I)) and  $1543\text{ cm}^{-1}$  (NH bending (amide II)) appeared. All the mentioned changes confirm attachment of the initiator to ITO surface.

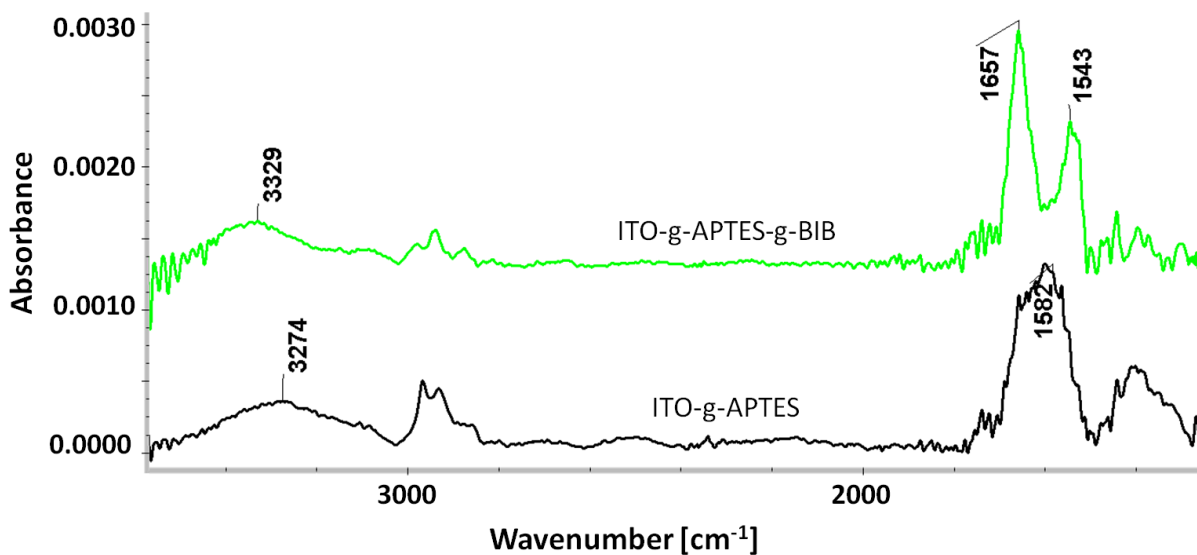


**Figure S20.** Grazing-angle FTIR spectra of ITO surface after subsequent APTES and BIB grafting.

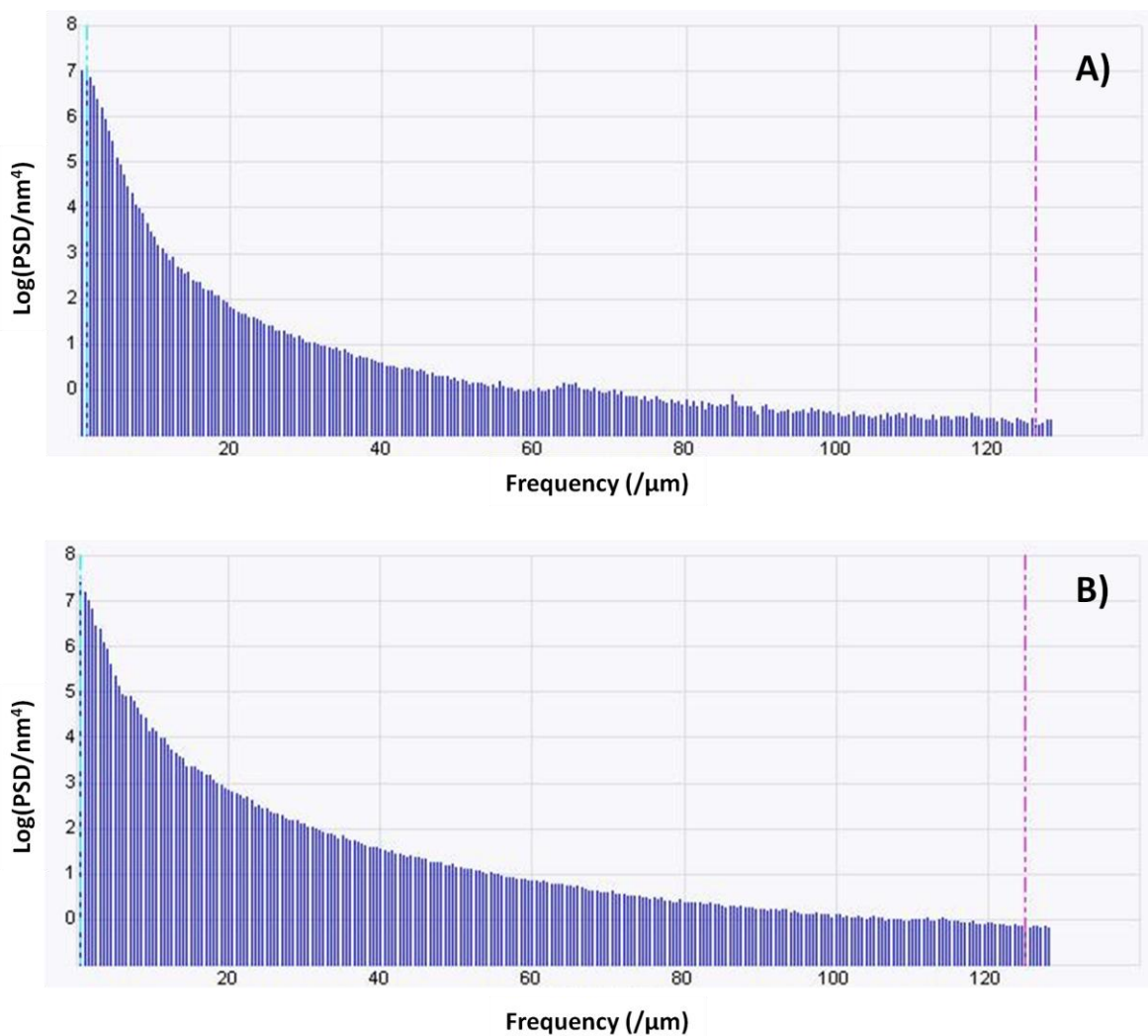


**Figure S21.** Power spectral density analysis performed for AFM images of PMTM<sub>60</sub> brushes after: A) SI-ATRP (see Figure 1B) and B) TBAF treatment (see Figure 1D).

2D isotropic power spectral density (2D PSD) profiles were calculated using the algorithm provided by the AFM software (Nanoscope). The presented 2D PSD profiles (see Figure S21) calculated from the AFM images of the PMTM\_60 brushes after SI-ATRP (based on Figure 1B) and after the subsequent TBAF treatment (based on Figure 1D) show no distinct peaks. Those observations indicate the lack of any regular isolated domains on the studied surfaces.